# Concentrated Phosphate Slurry Flow Simulations Using OpenFoam

**Souhail Maazioui**
Equipe Analyse des systèmes hydrauliques (EASH)
Ecole Mohammadia d'Ingénieurs,
Mohammed V University of Rabat, Morocco

Laboratoire Analyse, Géométrie et Applications (LAGA)
Université Sorbonne Paris Nord
Villetaneuse, France

Modeling Simulation & Data Analysis (MSDA)
Mohammed VI Polytechnic University Benguerir, Morocco
souhail.maazioui@um6p.ma

**Imad Kissami**
Modeling Simulation & Data Analysis (MSDA)
Mohammed VI Polytechnic University Benguerir, Morocco
Imad.kissami@um6p.ma

**Fayssal Benkhaldoun**
Laboratoire Analyse, Géométrie et Applications (LAGA)
Université Sorbonne Paris Nord
Villetaneuse, France
fayssal@math.univ-paris13.fr

**Abderrahim Maazouz**
IMP
Université de Lyon, INSA Lyon, Ingénierie des Matériaux Polymères
Villeurbanne, France
abderrahim.maazouz@insa-lyon.fr

**Driss Ouazar**
Equipe Analyse des systèmes hydrauliques (EASH)
Ecole Mohammadia d'Ingénieurs,
Mohammed V University of Rabat, Morocco
ouazar@emi.ac.ma

## Abstract

In this study, we seek to investigate the rheological behavior of phosphate suspension with the aim of performing numerical simulations of concentrated slurry flows using the open source framework OpenFoam. Adequate experimental protocols were presented to identify the main characteristics of these complex fluids and to establish relevant rheological models with a view to simulate numerical flow in a cylindrical pipeline. The solver nonNewtonianIcoFoam is used to compute slurry flows through an

axisymmetric pipe. For validation, the numerical results are compared to semi-analytical solutions for pipe flow of non-Newtonian fluids. It is shown that the axial velocity distribution and pressure loss computations using the incompressible non-Newtonian solver agree well with the semi-analytical results.

## Keywords
Rheology, Non-Newtonian Fluid, OpenFoam, Incompressible Flow

## 1. Introduction
Over the last two decades, the computational power has advanced rapidly and become a valuable tool to optimize and to improve complex flows transport and management. Engineers across a wide range of application and research areas rely henceforth on available Computational Fluid Dynamics (CFD) software packages to obtain a description of fluids flows at different levels of complexity. Different numerical methods and models for non-Newtonian incompressible flows were developed and implemented in many simulations software already. In this work, we seek to investigate the phosphate slurry flow using the open source framework OpenFoam which include a numerical solver for laminar non-Newtonian flow.

Our challenge here is to build a dynamic simulation model that can predict the performance of our system in the real world and to prevent dysfunction and problems such as clogs and to inform future decisions. From observations of the real world we build a mathematical model that can describe how the flow is currently moving to predict its future motion or position and speed at certain times. Two aspects are investigated: rheological model and transport model. Defining a rheological model allows us to determine the fluid flow that would be produced due to applied forces. This relation between deformation and stress must be included in the transport model to build an accurate simulation model that would match the observed behavior of the flow.

Rheology is a study of the change in form and flow of matter, primarily in a liquid state, embracing elasticity, viscosity and plasticity. It is used to describe the flow of non-Newtonian fluids and investigate the macroscopic behavior of complex fluids (suspensions, polymers, etc) under the action of stresses, deformations or underflow, widely present in the vast majority industrial processes. Understanding the behavior of fluids and complex fluids flow is of great interest as much from a fundamental point of view as from a point of industrial view.

The motivation behind this rheological study is the strong link between the transport characteristics of phosphate ore slurry and its rheological properties. In the design phase of a pipeline system, detailed knowledge of the rheological characteristics is essential for prediction of flow regime and head loss (Eshtiaghi et al., 2012). Concentrated slurries, that are mainly solid particles and suspending liquid mixtures, often display a variety of non-Newtonian flow properties, including shear thinning, shear thickening (Barnes, 1989; Maranzano et al., 2001). In piping systems, a shear-thinning slurry is often desired, where increasing the shear rate reduces the viscosity of the mixture, making the pumping system more efficient.

This research aims to present a methodology to exploit the rheological data obtained through experimental work in a practical way. This paper first describes the experiment procedure adopted for the rheological characterization of the concentrated phosphate slurry at the laboratory and gives an outlook on the behavior of yield pseudoplastics. In section 3, the authors describe the methodology of implementation of non-Newtonian rheological models in OpenFoam along with the procedure of running a simulation in the case of a laminar pipe flow. Finally, the paper ends with an outlook for future research and a thorough conclusion.

## 2. Experimental work
### 2.1 Materials

Phosphate ore is often mined at different locations, and then processed and mixed with water to be stored in agitated tanks before pumping through a pipeline. The samples used in this study are solid-liquid mixtures containing rigid randomly shaped solid particles with an equivalent spherical diameter ranging from 1µm to 500µm. Particle density is 2.4 t/m$^3$. Two samples, S1 and S2, with a phosphate ore concentrations of, respectively, 51% and 56% wt. in water are used for this rheological study. The solid particles contains mainly the elements $P_2O_5$ and CaO along with other elements such as $SiO_2$, $CO_2$, Fe, MgO, $SO_3$ and $Al_2O_3$.

## 2.1 Experimental data

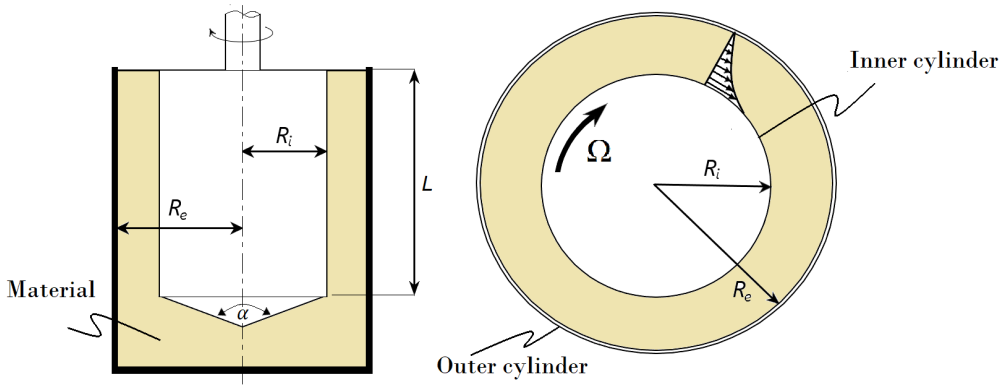


Figure 1. Searle principle: The instrument's motor rotates the measuring bob inside an immovable cup filled with slurry. $\alpha_{cyl.\ cone} = 120°$

The rheology of the phosphate slurry samples was measured using an Anton Paar RheolabQC rotational rheometer with a concentric cylinder, cf. Figure 1. Here, the Searle principle is considered, which is the most commonly used for mineral suspensions, with a rotating inner cylinder and stationary outer cylinder (Macosko, 1994; Schierbauni, 1964). Coaxial cylinder protocols are absolute measuring systems that conform to DIN and ISO. By measuring the rotational speed Ω of the electronically communicated (EC) motor and recording the resulting torque M, we are able to evaluate the shear stress $\tau$ and the shear rate $\dot{\gamma}$, at each measuring point Ω, according to the following relationships (Standard: ISO 3219 ($\delta \leq 1.2$)):

$$\dot{\gamma} = \frac{1+\delta^2}{\delta^2-1}\Omega \tag{1}$$

$$\tau = \frac{1+\delta^2}{2\delta^2} \cdot \frac{M}{2\pi\, L.R_i^2.C_L} \tag{2}$$

where $\delta = R_e/R_i$ is the ratio of the inner cylinder and outer cylinder radii, $R_e$ *and* $R_i$, $L$ is the bob length and $C_L = 1.28$ is an end effect correction factor.

Rheograms of these slurries were obtained by a preset shear rate ramp mode, descending in steps from 1000 $s^{-1}$ to 112 $s^{-1}$ and measuring the corresponding shear stress. The rotating bob and a cylindrical cup, have a diameter of 38.713 mm and 44 mm, respectively. The experimental data were obtained at room temperature. Before each measurement, the suspensions were vigorously mixed in a container to erase material memory and to have similar initial conditions for both samples and then poured quickly into the outer cylinder. Wall slip effects were not fully avoided using this geometry, therefore, any reproduction of the obtained rheograms has to be carried out carefully. The experimental data is reproduced in Figure 2. The rheological data in this study is retrieved from Maazioui et al., 2021.

For both samples, S1 and S2, rheograms reflect a non-Newtonian behavior with a non-zero intercept on the stress axis known as yield-pseudoplastic. The observed shear thinning was accentuated with higher solid concentration. Similarly, the dynamic yield stress increased with the increase of the solids concentration. As shown in Figure 2, the rheograms are accurately modeled with commonly used yield pseudoplastic models. The rheological parameters for the Bingham, Casson, Herschel-Bulkley, and Robertson-Stiff models have been computed for both samples and reported in Table 1. In the following, these rheological models are defined.

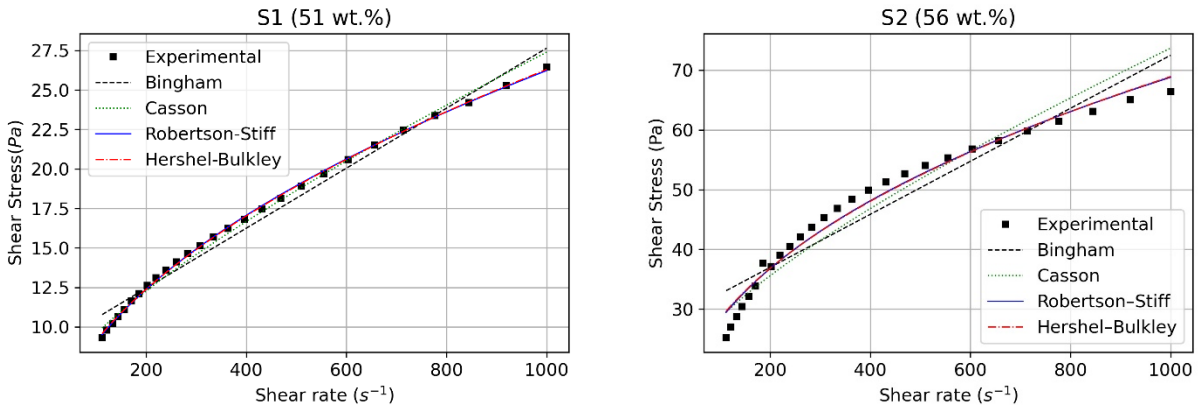


(**a**) (**b**)

Figure 2. Rheograms and comparison of rheological models fitting for (a) S1 and (b) S2

For Newtonian fluids, shear stress is a linear relation of the shear rate:

$$\tau = \mu\dot{\gamma} \tag{3}$$

where μ is the constant viscosity of the fluid. Non-Newtonian fluids show a different behavior where an apparent viscosity η is often assigned:

$$\tau = \eta(\dot{\gamma})\dot{\gamma} \tag{4}$$

For yield pseudoplastic fluids, the have an interesting feature that can be expressed by:

$$\dot{\gamma} = 0, |\tau| < \left|\tau_y\right|, \tag{5}$$

where $\tau_y$ represent the yield stress. The most known representation of these complex fluids is the Bingham model (Bingham, 1916) given by the following equation:

$$\tau = \tau_{yB} + \eta_B\dot{\gamma} \tag{6}$$

where, $\tau_{yB}$ is the yield stress and $\eta_B$ is the constant plastic viscosity. The Herschel-Bukley model (Herschel, 1924) can be expressed with the following constitutive equation:

$$\tau = \tau_{yH} + K\dot{\gamma}^n \tag{7}$$

where $\tau_{yH}$ represents the dynamic yield stress, $K$ is the consistency index, and $n$ is the flow index. The Casson model (Casson, 1959) is given by the following equation:

$$\sqrt{\tau} = \sqrt{\tau_{yc}} + \sqrt{k_c}\sqrt{\dot{\gamma}} \tag{8}$$

The Robertson–Stiff model (Ohen et al., 1990) is also a three-parameter model and it is expressed as:

$$\tau = K(\dot{\gamma} + \dot{\gamma}_0)^n \tag{9}$$

where the yield stress is defined as:

$$\tau_{yRS} = K\dot{\gamma}_0^n \tag{10}$$

Equation 5 inherits a discontinuity at the limit of the plug zone, where $\dot{\gamma} = 0$, that was dealt with by Papanastasiou, 1987, by introducing an exponential function to the Bingham model. The corresponding viscosity can be written as follows:

$$\mu_{e,\epsilon} = \mu + \frac{\tau_y}{\dot{\gamma}}(1 - e^{-\dot{\gamma}m}) \tag{11}$$

To evaluate the fitting capabilities of each model, the following statistical indicators were computed and reported in Table 2: the correlation coefficient, $R^2$, the sum of square errors, SSE, and the root mean square error, RMSE.

Table 1. Constant parameters for rheological models

| Model | Rheological parameters | samples | |
|---|---|---|---|
| | | S1 | S2 |
| Bingham | $\tau_{yB}$ , Pa | 5.54 | 18.92 |
| | $\eta_B$ , Pa.s | 0.024 | 0.061 |
| Casson | $\tau_{yc}$ , Pa | 4.42 | 14.8 |
| | $\eta_c$ , Pa.s | 0.01 | 0.022 |
| H-B | $\tau_{yH}$ , Pa | 1.36 | 3.7 |
| | $K$, Pa.s$^n$ | 0.75 | 3.56 |
| | $n$ | 0.51 | 0.42 |
| R-S | $K$, Pa.s$^n$ | 0.99 | 4.56 |
| | $n$ | 0.47 | 0.39 |
| | $\dot{\gamma}_0$ , s$^{-1}$ | 6.63 | 3.7 |
| | $\tau_{yRS}$, Pa | 2.40 | 7.5 |

Table 2. Statistical indicators

| Model | Statistical indicators | samples | |
|---|---|---|---|
| | | S1 | S6 |
| Bingham | $R^2$ | 0.97 | 0.9 |
| | SSE | 12.16 | 356.49 |
| | RMSE | 0.67 | 3.63 |
| Casson | $R^2$ | 0.99 | 0.93 |
| | SSE | 3.94 | 252.25 |
| | RMSE | 0.38 | 3.05 |
| H-B | $R^2$ | 0.99 | 0.97 |
| | SSE | 0.48 | 93.8 |
| | RMSE | 0.13 | 1.86 |
| R-S | $R^2$ | 0.99 | 0.97 |
| | SSE | 0.52 | 86.74 |
| | RMSE | 0.14 | 1.79 |

The Robertson-Stiff (R-S) and Herschel-Bulkley (H-B) models provided the best fit for both samples with correlation coefficients $R^2$ ranging from 0.97 to 0.99. With the use of a third parameter in the rheological model, we often obtain a better fit to experimental data. However Bingham model has yielded acceptable fitting capabilities. Thus, for the sake of simplicity, this article will be limited to the description of the numerical simulations using Papanasasiou model, the regularized Bingham model. Other models can be implemented, practically, in the same manner.

## 3. Methods

OpenFOAM is an open source software for computational fluid dynamics (CFD) representing a C++ toolbox for the development and use of numerical solvers and pre-/post-processing utilities intended for the solution of continuum mechanics applications. OpenFoam v8 includes three solvers for the flow of non-Newtonian fluids. The three solvers are listed below:

- SimpleFoam, a steady state solver for incompressible, turbulent flow of non-Newtonian fluids.
- nonNewtonianIcoFoam, a transient solver for incompressible and laminar flow of non-Newtonian fluids.
- PISOFoam, a transient solver for incompressible and turbulent flow of non-Newtonian fluids.

Non-Newtonian solvers can be found at:

$FOAM_SOLVERS/incompressible

### 3.1 nonnewtonianIcoFoam

OpenFOAM has pre-built object-oriented library for simulating the laminar flow of non-Newtonian fluids, which is nonNewtonianIcoFoam. Considering an unsteady incompressible flow for both Newtonian and nonNewtonian, the governing equations solved in nonNewtonianIcoFoam solver can be describe with the following conservation equations of mass and momentum:

$$\nabla \cdot U = 0 \tag{12}$$

$$\frac{\partial U}{\partial t} + \nabla .(UU) = -\nabla p + \nabla \cdot (\nu(D)(\nabla U + \nabla U^T)) \tag{13}$$

Where $U$ is the material velocity and $p$ the pressure field. The kinematic viscosity $\nu = \eta/\rho$ is described with the one of the rheological models presented in Eqs. 5-9. We note that the rate of strain in Eq. 11 is expressed as follows:

$$D = \frac{1}{2}(\nabla u + (\nabla u)^T) \tag{11}$$

nonNewtonianIcoFoam is based on PISO algorithm (Issa, 1986) which stands for Pressure-Implicit with splitting of Operators. PISO algorithm is used for the pressure-velocity coupling in unsteady cases. The discretized form of Eq. 10 and 11 present a linear dependence of velocity field on pressure field. This pressure-velocity coupling requires a special treatment. Issa 1986 proposed a efficient method of dealing with the pressure-velocity coupling system. For further reading, we refer to the work by Jasak, 1996.

### 3.2 Non-Newtonian rheological models

The framework OpenFOAM provides a library of viscosity models ν including Bingham, Herschel-Bukley, Casson. The rheological models are expressed in term of the strain rate $\dot{\gamma}$ and can be specified by the user in the transportProperties dictionary. As mentioned in Eq. 11, the strain rate can be formulated in OpenFoam as:

$$strain\ Rate = \sqrt{2 * symm\big(grad(U)\big) : symm(grad(U))}$$

where

$$symm\big(grad(U)\big) = grad(U) + grad(U).T$$

The shear strain rate function, strainRate(), is located in viscosityModel class which is defined in viscosityModel.C

```
Foam::tmp<Foam::volScalarField> Foam::viscosity Model::strainRate()
const
{
return sqrt(2.0)*mag(symm(fvc::grad(U_)));
}
```

To implement the Papanastasiou model (Eq. 10) in transportProperties dictionary, we define the model in Papanastasiou.C as below, and then we create the corresponding Make/files and Make/options.

```
Foam::tmp<Foam::volScalarField>
Foam::viscosityModels::Papanastasiou::calcNu() const
{
      return   (scalar(1)-exp(m_* strainRate ()))*(tau0_ +
k_*pow(strainRate());
, n_))/(max(strainRate());
, dimensionedScalar ("vSmall", dimless/dimTime, vSmall)));

}
```

### 3.3 Test case

The present test case simulation was performed using OpenFOAM v8. Yield pseudoplastic flow is solved with nonNewtonianIcoFoam solver. The above stated non-Newtonian Papanastasiou transport model was implemented in the transportProperties dictionary and considered as rheological model in this test case. Velocity field is solved with the smoothSolver with a corresponding symGaussSeidel smoother and pressure is solved with the Geometric agglomerated Algebraic MultiGrid preconditioner (GAMG). It is worth mentioning that the gravity force is not considered in this problem. Also, the physical properties of the fluid are assumed to be constant except for the viscosity.

We assess our method based on a axisymmetric unsteady pipe flow test as shown below in the schematic diagram of the numerical domain in Figure 3. Regarding the boundary conditions, the flow velocity is constant in axial direction at the inlet and a zeroGradient condition is applied for pressure. At the outlet, zeroGradient is set for velocity and a fixed value is given for pressure. Standard no-slip condition is applied at the pipe wall.

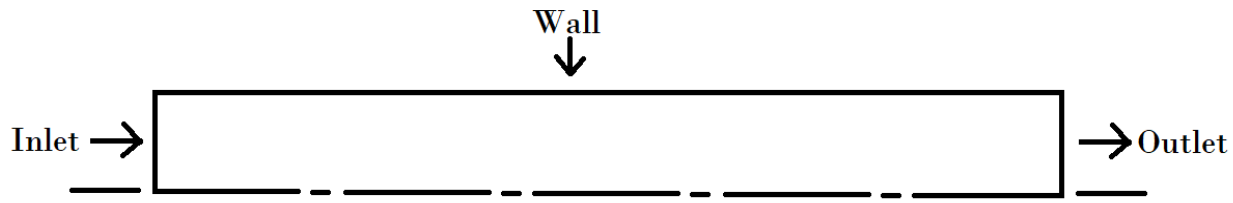


Figure 3. 2D axysymmetrical pipe flow schematic diagram

With the assumption of an unidirectional and axisymmetric flow of a fluid through in a circular pipe of radius $R$, it is possible to express the volumetric flow rate $Q$ in function of the pressure gradient $\Delta p/L$ and the rheological parameters. If the flow is fully-developed, we obtain the well known Rabinowitsch-Mooney equation:

$$\frac{Q}{\pi R^3} = \frac{1}{\tau_w^3}\int_0^{\tau_w} \tau^2 \dot{\gamma}\, d\tau, \tag{15}$$

where $\tau_w$ is the wall shear stress given by:

$$\tau_w = \frac{R}{2}\frac{\Delta p}{L}, \tag{16}$$

To obtain explicit expressions of Eq. 15, we substitute $\dot{\gamma}$ with the algebraic expressions of the rheological models, allowing the integral to be evaluated analytically. This applies in the same manner for cross-sectional velocity profiles for a given pressure drop. The shear rate is defined by as:

$$\dot{\gamma} = du/dr \tag{17}$$

By assuming a no-slip condition $u(R) = 0$ and integrating Eq. 17, we can write the cross-sectional velocity profile in the axial direction u(r):

$$u(r) = \int_r^R \dot{\gamma}\, dr, \tag{17}$$

# 4. Results and Discussion

## 4.1 Numerical Results

As expected, the numerical results of the performed test cases reveal that the yield pseudoplastics fluids show a plug flow region at the center of the pipe. In addition, using different viscosity parameters, leads to significant changes in the behavior of the incompressible pipe flow. Figures 4-5 show the simulation results for both sample S1 and S2, respectively.


Figure 4. Velocity field U for sample S1 using Papanastasiou model


Figure 5. Velocity field U for sample S2 using Papanastasiou model

By applying an inlet velocity of 1 m/s, we can compute the resulting pressure loss throughout the pipe. The simulations yields the following pressure loss results for S1 and S2 (see Figure 6).

- S1 : $\Delta p/L = 25.6\ Pa,$ for a mass flow rate of $\dot{m} = 1200\ kg/s$
- S2 : $\Delta p/L = 85\ Pa,$ for a mass flow rate of $\dot{m} = 1256\ kg/s$

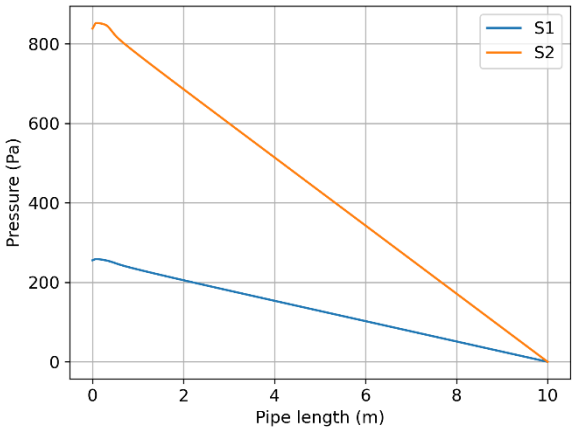


Figure 6. Pressure loss along the pipe for S1 and S2

The rheology of slurries is a function of its physical properties. The most important factors are the particle volume fraction, particle shape, interactions between particles, and the spatial arrangement of particles. Here, sample S2 has a higher solid concentration in comparison with sample S1. Therefore, the rheology of S2 is much higher than S1, and as a consequence, we need more power to pump it due to the frictional losses throughout the pipe, Maazioui et al., 2021.

## 4.2 Validation

In order to validate the accuracy of numerical solution, the numerical results can be compared with the results of the semi-analytical solution described in section 3.4. A typical benchmark test case for an implemented computational non-Newtonian application is the flow through a cylindrical pipe. The advantage of that case is the existing semi-analytical solution obtained from the simplified Navier-Stokes equations (Eq. 12-13). The velocity profiles are calculated using the resulting pressure loss of the numerical solutions as input.

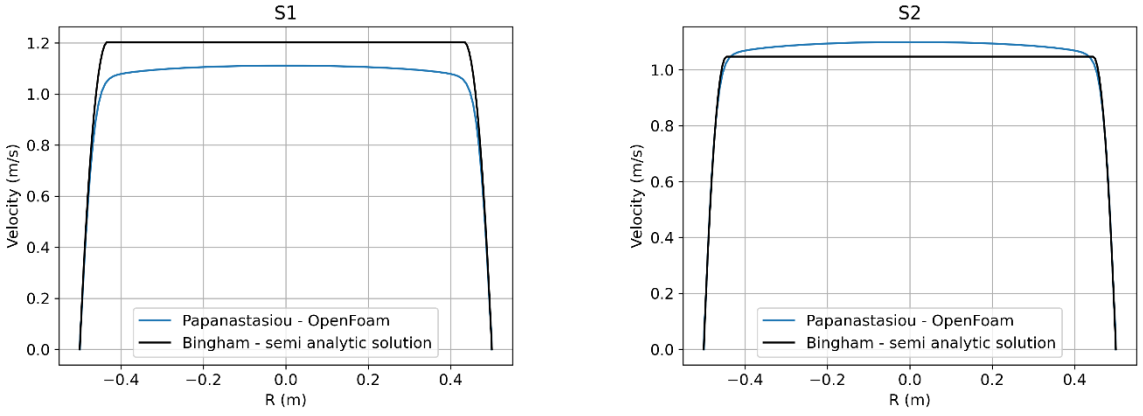


(**a**) (**b**)

Figure 7. Comparaison between numerical results and semi analytical results for (a) S1 and (b) S2

Figure 7 illustrates the cross section velocity profiles for both samples S1 and S2 in comparison with the resulting velocity profile using semi-analytical formulas. As can be seen in Figure 7, the numerical method predicts velocity profiles and pressure losses that are in good agreement with the analytical solutions. In all, numerical investigation of

concentrated phosphate slurry seems to be a suitable tool and control to design and control the phosphate ore transport in pipelines systems.

## 5. Conclusion

The main target of the presented work was to perform Non-Newtonian flows simulations using the open source computational framework OpenFOAM. The rheological model according to Papanastasiou was implemented in transport models library of OpenFOAM. The rheological data was collected from the results of experimental procedures for concentrated phosphate slurry rheological characterization. Results show that the required energy for pumping depends on the rheological characteristic of the transported material. Additionally, the solutions of our simulation method is compared with the results of semi analytical method, which shows that CFD computations can be very useful at an industrial level. These findings can be exploited for a better control of concentrated phosphate slurries, which allow the mineral industry to improve its logistic chain.

## References

Barnes, H. A. (1989). Shear-thickening ("Dilatancy") in suspensions of nonaggregating solid particles dispersed in Newtonian liquids. *Journal of Rheology*, *33*(2), 329-366.

Bingham, E. C. (1916). An investigation of the laws of plastic flow. Bul Bur Standards 13: 309-353.

Casson, N. (1959). A flow equation for pigment-oil suspensions of the printing ink type. *Rheology of disperse systems*.

Eshtiaghi, N., Markis, F., & Slatter, P. (2012). The laminar/turbulent transition in a sludge pipeline. *Water Science and Technology*, *65*(4), 697-702.

Herschel, W. H. (1924). Consistency of rubber benzene solutions. *Industrial & Engineering Chemistry*, *16*(9), 927-927.

ISO, E. (1993). Plastics—Polymers/resins in the liquid state or as emulsions or dispersions—Determination of viscosity using a rotational viscometer with defined shear rate (ISO).

Issa, R. I. (1986). Solution of the implicitly discretised fluid flow equations by operator-splitting. *Journal of computational physics*, *62*(1), 40-65.

Jasak, H. (1996). Error analysis and estimation for the finite volume method with applications to fluid flows.

Maazioui, S., Maazouz, A., Benkhaldoun, F., Ouazar, D., & Lamnawar, K. (2021). Rheological Characterization of a Concentrated Phosphate Slurry. *Fluids*, *6*(5), 178

Macosko, C. W. (1994). Rheology Principles. *Measurements and Applications*.

Maranzano, B. J., & Wagner, N. J. (2001). The effects of particle size on reversible shear thickening of concentrated colloidal dispersions. *The Journal of chemical physics*, *114*(23), 10514-10527.

Ohen, H. A., & Blick, E. F. (1990). Golden section search method for determining parameters in Robertson-Stiff non-Newtonian fluid model. *Journal of Petroleum Science and Engineering*, *4*(4), 309-316.

Papanastasiou, T.C. Flows of materials with yield. J. Rheol. 1987, 31, 385–404

Schierbauni, F. (1964). Wazer, JR van, JW Lyons, KY Kim und RE Colwell: Viscosity and flow measurement. A laboratory handbook of rheology. 1963 Interscience Publishers, a division of John Wiley and Sons, New York, London. XX, 406 Seiten mit zahlreichen Abb. u. Tab., Gr.− 8°, geb., Preis 103 s.